Bulgarian Chemical Communications, Volume 50, Special issue H (pp. 87–92) 2018

Synthesis, structure, and catalytic properties of $SrFe_{12}O_{19}$ hexaferrite

K. V. Koleva[1]*, N. I. Velinov[1], I. G. Genova[2], T. S. Tsoncheva[2], V. S. Petkova[3,4]

[1] *Institute of Catalysis, Bulgarian Academy of Sciences, 1113 Sofia, Bulgaria*
[2] *Institute of Organic Chemistry with Centre of Phytochemistry, Bulgarian Academy of Sciences, 1113 Sofia, Bulgaria*
[3] *Institute of Mineralogy and Crystallography, Bulgarian Academy of Sciences, 1113 Sofia, Bulgaria*
[4] *New Bulgarian University, Department of Natural Sciences, 21 Montevideo St., 1618 Sofia, Bulgaria*

Received: January 16, 2018; Revised, March 15, 2018

M-type $SrFe_{12}O_{19}$ hexaferrites were synthesised by means of co-precipitation method followed by annealing at 600 °C and 850 °C. A portion of a sample, treated at 850 °C, was further subjected to high-energy ball milling for 1 and 5 hours. TG-DTG-DTA, X-ray powder diffraction, and ^{57}Fe Mössbauer spectroscopy were used for samples characterisation. A well-crystallised $SrFe_{12}O_{19}$ hexaferrite phase and small amount of secondary hematite (α-Fe_2O_3) phase were observed after annealing at 850 °C. Changes in the structure and a decrease in crystallite size of $SrFe_{12}O_{19}$ from 47 nm to 22 nm were observed after one-hour ball-milling treatment. Prolongation of the milling time induced separation of hematite phase and the highest amount was achieved after 5 hours of treatment. All samples exhibited good catalytic activity and CO selectivity in methanol decomposition. Mössbauer study of catalytically tested materials demonstrated stability of the hexaferrite phase under reductive reaction conditions.

Key words: M-type hexaferrites, Mössbauer spectroscopy, methanol decomposition.

INTRODUCTION

Hexaferrite materials are in the focus of many investigations due to their superior electrical and magnetic properties. The M-type $SrFe_{12}O_{19}$ hexaferrite material has hexagonal crystal structure of $P6_3$/mmc space group. This structure is built by divalent alkaline earth metals, such as Sr, Ca or Ba, and Fe^{3+} ions that occupied tetrahedral (4f1), octahedral (12k, 2a, 4f2), and hexahedral (2b) crystallographic sites in the oxygen lattice.

Different methods for preparation of hexaferrite powders, such as sol-gel [1], sol-gel auto combustion [2], glass ceramic [3], hydrothermal synthesis [4], co-precipitation [5], and ball milling [6−8] have been reported. Among them ball-milling procedures provide the production of powders, consisting of fine particles, being smaller than the single-domain size, by simple operation and handy experimental equipment [9].

Catalytic processes successfully solve a number of contemporary problems related to environmental and energy demands. Recently, methanol decomposition has received much attention as a potential source of clean and efficient fuel for gas turbines, fuel cells, and vehicles [10−12]. Morphology and structure features of metal oxide materials with spinel structure regarding their catalytic behaviour in methanol decomposition have already been reported [13−16]. To the best of our knowledge, studies of strontium hexaferrites materials as catalysts for methanol decomposition have not been published so far.

The goal of the present work was to synthesise $SrFe_{12}O_{19}$ hexaferrite materials of tunable particle size using the method of mechanochemical treatment. Synthesis parameters impact on catalytic activity and selectivity of the obtained materials in methanol decomposition is in the focus of the study.

EXPERIMENTAL

Synthesis

$SrFe_{12}O_{19}$ samples were synthesised by co-precipitation method followed by thermal treatment. $Sr(NO_3)_2$ and $Fe(NO_3)_3.9H_2O$ supplied by Alfa Aesar were used as starting materials at an appropriate molar ratio. A mixed nitrate solution was precipitated dropwise by NaOH. The precipitate was dried at room temperature to form a precursor powder. The thermal treatment was carried out in static air at two temperatures: 600 and 850 °C with a hold of four hours. After heating at 850 °C, the powder was milled for 1 and 5 hours using a Fritsch Planetary miller in a hardened steel vial together with fifteen grinding balls of diameters ranging from 3 to 10 mm. The balls-to-powder mass ratio was 10:1. The abbreviations used in sample names are: HF – hexaferrite, TS – thermal synthesis, MS – mechano-che-

---

* To whom all correspondence should be sent
E-mail: kremena_vassileva@abv.bg

mical synthesis, and MD – after methanol decomposition.

Characterisation

Dried precursor powders (HC) were analysed by thermogravimetry and differential thermal analysis (TG-DTA) using a Stanton Redcroft instrument in static air at a heating ramp rate of 10 °C/min. Powder X-ray diffraction (XRD) samples were recorded by use of a TUR M62 diffractometer with Co Kα radiation. Average crystallite size (D, nm), degree of microstrain (e), and lattice parameters (a) of the studied hexaferrites were calculated from experimental XRD profiles by using PowderCell-2.4 software [17]. The Mössbauer spectra were registered at room temperature (RT) on a Wissel (Wissenschaftliche Elektronik GmbH, Germany) electromechanical spectrometer working in a constant acceleration mode. A $^{57}Co/Rh$ (activity ≅ 50 mCi) source and an α-Fe standard were used. Experimentally obtained spectra were fitted using CONFIT2000 software [18]. Parameters of hyperfine interactions, such as isomer shift (IS, mm/s), quadrupole splitting (QS, mm/s), effective internal magnetic field (H_{eff}, T), line widths (FWHM, mm/s), and relative weight (G, %) of the partial components in the spectra were determined.

Catalytic test

Methanol decomposition was carried out in a flow reactor at methanol partial pressure of 1.57 kPa and argon as a carrier gas (50 ml/min). The catalysts (0.055 g) were tested under temperature-programmed regime within the range of 77−500 °C at a heating ramp rate of 1 °C/min. On-line gas chromatographic analyses were performed on a PLOT Q column using flame ionisation and thermal conductivity detectors. An absolute calibration method and a carbon based material balance were used to calculate conversions and yields of the obtained products. Products selectivity was calculated as $Y_i/X*100$, where Y_i is the current yield of product i and X is methanol conversion.

RESULTS AND DISCUSSION

TG-DTG-DTA analysis of dried precursor powder is shown in Fig. 1. A significant endo-thermal effect up to 400 °C combined with sample mass loss could be associated with dehydration. Two exothermal peaks at 576 and 820 °C are due to crystallisation of hematite and hexaferrite phase, respectively [19,20].

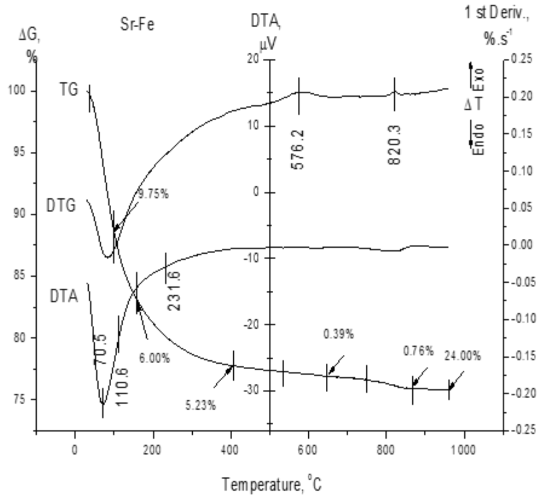

Fig. 1. TG-DTG-DTA investigation of $SrFe_{12}O_{19}$ dried precursor sample.

Powder X-ray diffraction patterns of heat-treated and ball-milled $SrFe_{12}O_{19}$ samples are shown in Fig. 2. In accordance with DTA analysis, diffractions of the precursor powder and of the sample obtained at 600 °C correspond to hematite - α-Fe_2O_3 (S.G.: R3c). Well defined reflexes of highly crystalline $SrFe_{12}O_{19}$ (Fig. 2b) were registered after 4-h treatment at 850 °C (ICDD, PDF 80-1198). Calculated average crystallite size, microstrain degree, and lattice parameters are given in Table 1.

Table 1. Average crystallites size (D), degree of microstrain (e) and lattice parameters determined from XRD patterns of $SrFe_{12}O_{19}$.

Sample	Phases	D, nm	e 10^3 a.u	a, c, Å		%
HF TS850	$SrFe_{12}O_{19}$	47.38	1.14	a = 5.87	c = 23.04	93
	α-Fe_2O_3	66.58	1.26	a = 5.03	c = 13.73	7
HF TS850/MS1	$SrFe_{12}O_{19}$	24.98	5.67	a = 5.87	c = 23.04	88
	α-Fe_2O_3	35.83	1.66	a = 5.02	c = 13.72	12
HF TS850/MS5	$SrFe_{12}O_{19}$	25.07	7.81	a = 5.87	c = 23.13	57
	α-Fe_2O_3	25.03	5.63	a = 5.04	c = 13.75	43

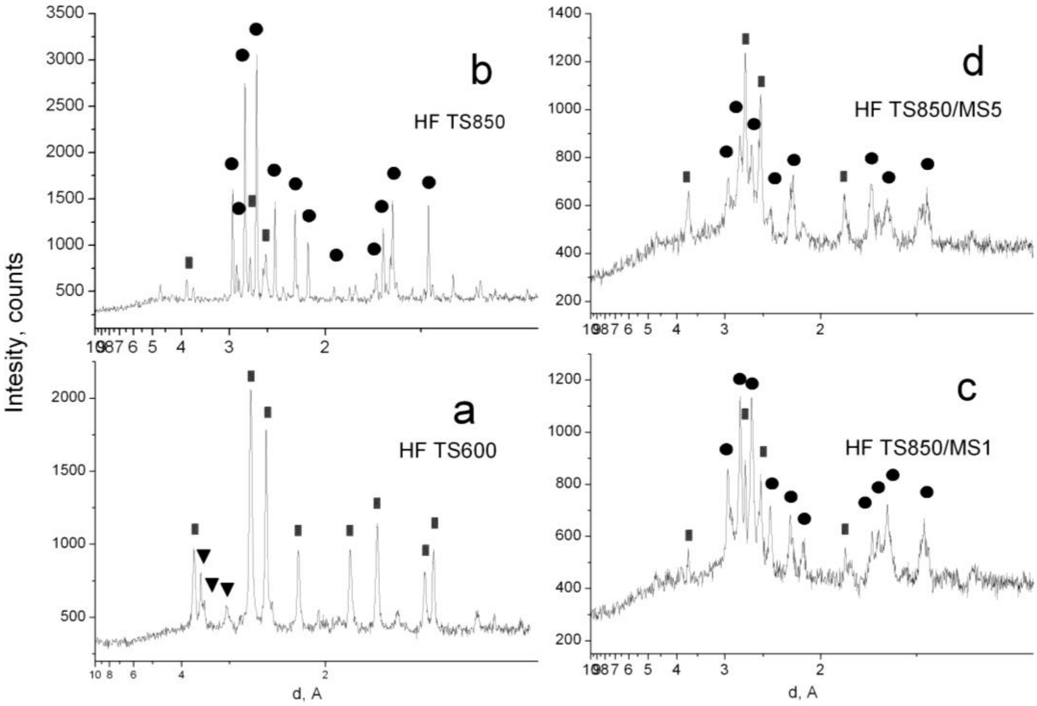

Fig. 2. X-ray analysis of thermally synthesised (a, b) and mechanochemically obtained (c, d) SrFe$_{12}$O$_{19}$ samples (●- SrFe$_{12}$O$_{19}$, ■- α-Fe$_2$O$_3$ and ▼-SrCO$_3$).

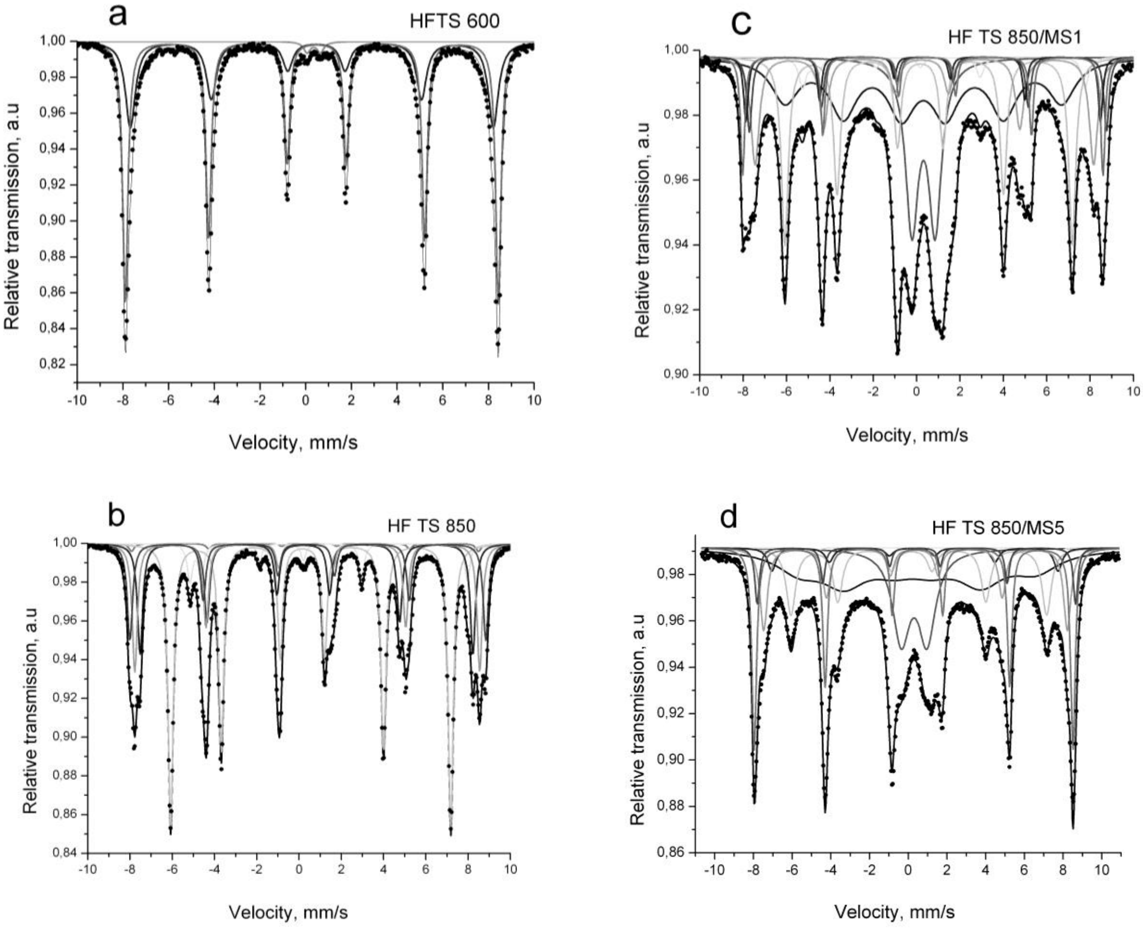

Fig. 3. Mössbauer spectra of thermally (a, b) and mechanochemically (c, d) synthesized SrFe$_{12}$O$_{19}$ samples.

Table 2. Mössbauer parameters of $SrFe_{12}O_{19}$ samples.

Sample	Components	IS, mm/s	QS, mm/s	Heff, T	FWHM mm/s	G, %
HF TS600	Sx1 Fe_2O_3	0.37	-0.21	50.7	0.28	64
	Sx2 Fe_2O_3	0.36	-0.20	49.3	0.53	35
	Db	0.34	0.58	-	-	1
HF TS850	octahedral (4f2)	0.38	0.07	52.3	0.30	14
	octahedral (2a)	0.35	0.06	50.7	0.29	17
	tetrahedral (4f1)	0.27	0.15	48.9	0.30	18
	octahedral (12k)	0.35	0.39	41.2	0.29	44
	bipyramidal (2b)	0.28	2.23	40.8	0.29	6
	Fe_2O_3	0.38	-0.20	51.0	0.29	1
HF TS850/MS1	octahedral (4f2)	0.45	0.14	51.2	0.28	6
	octahedral (2a)	0.28	0.04	50.8	0.25	4
	tetrahedral (4f1)	0.30	0.12	48.5	0.47	13
	octahedral (12k)	0.36	0.38	41.2	0.39	21
	bipyramidal (2b)	0.20	2.10	40.5	0.40	3
	Sx	0.31	0.27	39.7	1.60	30
	Db	0.31	1.07	-	0.72	16
	Fe_2O_3	0.38	-0.20	51.6	0.23	7
HF TS850/MS5	octahedral (4f2)	0.38	0.07	51.1	0.28	5
	octahedral (2a)	0.34	0.06	48.7	0.46	12
	tetrahedral (4f1)	0.27	0.15	45.9	0.50	4
	octahedral (12k)	0.36	0.36	41.1	0.57	13
	bipyramidal (2b)	0.28	2.20	40.7	0.30	1
	Sx	0.35	0.27	38.0	2.85	30
	Db	0.29	1.33	-	1.07	16
	Fe_2O_3	0.37	-0.20	51.2	0.29	19
HF TS850MD	octahedral (4f2)	0.38	0.09	52.1	0.35	15
	octahedral (2a)	0.36	0.06	50.5	0.33	20
	tetrahedral (4f1)	0.27	0.15	48.8	0.30	15
	octahedral (12k)	036	0.39	41.1	0.30	44
	bipyramidal (2b)	0.29	2.21	40.6	0.28	6
HF TS850/MS1MD	octahedral (4f2)	0.39	0.09	51.3	0.40	8
	octahedral (2a)	0.33	0.05	50.1	0.36	12
	tetrahedral (4f1)	0.30	0.06	48.4	0.43	19
	octahedral (12k)	0.36	0.38	40.9	0.32	17
	bipyramidal (2b)	0.23	2.07	40.5	0.30	3
	Sx	0.33	0.07	40.2	1.38	41
HF TS850/MS5MD	octahedral (4f2)	0.37	0.07	50.6	0.30	4
	octahedral (2a)	0.35	0.06	48.7	0.40	8
	tetrahedral (4f1)	0.27	0.15	46.7	0.80	13
	octahedral (12k)	0.37	0.33	40.6	0.66	18
	bipyramidal (2b)	0.28	2.20	41.2	0.30	1
	Sx	0.35	0.14	34.3	1.54	21
	Fe_2O_3	0.38	-0.20	50.9	0.38	35

Significant transformations with the $SrFe_{12}O_{19}$ TS850 sample occurred after mechanochemical activation (Fig. 2c and d, and Table 1). Even after 1-h ball milling a decrease of the crystallite size from 47 nm to 24 nm and an increase of the microstrain degree from 1.14×10^{-3} to 5.67×10^{-3} were observed. Increasing the milling time up to five hours resulted in the appearance of almost 50% secondary hematite phase.

Mössbauer spectra of the obtained samples and matching calculated parameters are given in Fig. 3 and Table 2, respectively. In the case of HF TS600 the best fitting model consists of two sextet components and a doublet with IS = 0.34 mm/s and QS = 0.58 mm/s parameters indicating presence of amorphous phase. The appearance of more than one sextet component is associated with hematite phase of different particle size. M-type $SrFe_{12}O_{19}$ was detected after a temperature rise up to 850°C. The spectrum represented five well visible magnetically split components, indicating different cation environment around the Fe^{3+} ion in the hexagonal structure S.G.: $P6_3/mmc$ [21]. The sextet parameter of the lowest IS (IS = 0.27 mm/s) is due to iron ion in tetrahedral position (FeO_4), while the component with the largest QS (around 2.20 mm/s) is typical of a site of the lowest symmetry - trigonal bipyramidal [22]. Octahedrally coordinated Fe^{3+} are described as 4f2, 2a and 12k Wyckoff positions. Results from Mössbauer spectroscopy show a change in the material that occurred within one hour of milling. The observed collapse in the magnetic hyperfine structure in this case indicated significant changes in the sample. Appearance of additional magnetically split component with large width (FWHM = 1.6 and 2.85 mm/s for 1 and 5 hours milling, respectively) could be due to formation of highly defective and finely divided hexaferrite particles [23]. After mechanical activation, the appearance of non-magnetic component in the spectrum is evidence for the formation of highly dispersed material as well. About 16% of the total spectral area represents a doublet with parameters of the Fe^{3+} oxidation state, due to superparamagnetism phenomenon [24]. Thus, a short time grinding provides reduction in the particles size of less than 10 nm. Elongation of milling time induced separation of hematite phase.

All materials were catalytically active in methanol decomposition above 300 °C and at 350 °C about an 80–100% conversion was achieved. According to their catalytic activity, the samples arrange in the following order: HF TS850 < HF TS850 MS1 < HF TS850 MS5 (Fig. 4).

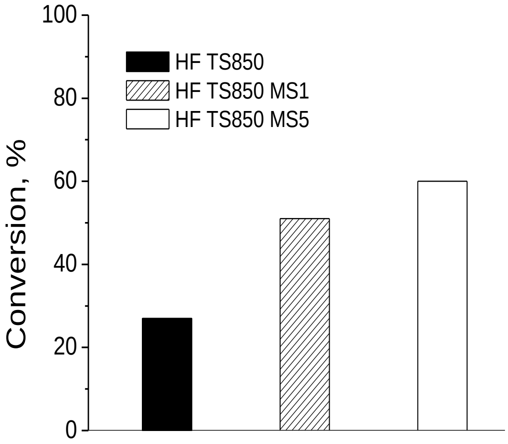

Fig. 4. Methanol decomposition at 330 °C on various samples.

For all materials, the selectivity to CO was about 80% and CO$_2$ and methane were registered as by-products. After catalysis, Mössbauer analysis of the samples was carried out. Parameters of hyperfine interaction are presented in Table 2. Despite strong reductive reaction atmosphere, no changes in phase composition of the initial materials were observed. None second hematite phase was registered only in the case of HF TS 850. A missing doublet component in the spectra of the milled samples indicates particle aggregation during the catalytic reaction.

CONCLUSIONS

Nanocrystalline M-type SrFe$_{12}$O$_{19}$ hexaferrite was successfully synthesised by thermal method combined with a ball-milling procedure. Powder X-ray diffraction and ^{57}Fe Mössbauer spectroscopy analyses indicated a facile effect of shorter milling time on the formation of homogeneous and finely divided SrFe$_{12}$O$_{19}$ hexaferrite and an increase of second hematite phase. The ball-milling procedure enhanced the catalytic activity of the samples in methanol decomposition and no significant effect of the milling time was detected. Mössbauer study of the catalysts after tests indicated that the hexaferrite phase remained stable even under highly reductive conditions.

Acknowledgment: *Financial support by the Bulgarian Academy of Sciences under project 'Advertisements and competitions for young scientists and scholars' (DFNP 17-34) is gratefully acknowledge.*

REFERENCES

1. J. Qiu, L. Lan, H. Zhang, M. Gu, *J. Alloys Compd.*, **453**, 261 (2008).
2. A. Baykal, S. Yokuş, S. Güner, H. Güngüneş, H. Sözeri, Md. Amir, *Ceram. Int.*, **43**, 3475 (2017).
3. J. H. de Araur, F. A. O. Cabral, M. F. Ginani, J. M. Soares, F. L. A. Machado, *J. Non-Cryst. Solids,* **352**, 3518 (2006).
4. L. Lechevalliera, J. M. Le Breton, J. F. Wangc, I. R. Harris, *J. Magn. Magn. Mater.*, **269**, 192 (2004).
5. V. Luna, S. A. Palomares-Sanchéza, F. Ruíza, *Catal. Today*, **266**, 110 (2016).
6. I. Bsoul, S. Mahmood, A. F. Lehlooh, *Alloys Compd*., **498**, 157 (2010).
7. I. Bsoul, S. Mahmood, *J. Alloys Compd.*, **489**, 110 (2010).
8. I. Bsoul, S. Mahmood, *Jordan J. Phys.*, **2**, 171 (2009).
9. A. Awadallaha, S. H. Mahmooda, Y. Maswadeha, I. Bsoulb, M. Awawdehc, Q. I. Mohaidatc, H. Juwharia, *Mater. Res. Bull.*, **74**, 192 (2016).
10. M. Ni, D. Y. C. Leung, M. K. H. Leung, *Int. J. Hydrogen Energy*, **32**, 3238 (2007).
11. H. Muroyama, R. Nakase, T. Matsui, K. Eguchi, *Int. J. Hydrogen Energy*, **35**, 1575 (2010).
12. F. Frusteri, S. Freni, L. Spadoro, V. Chiodo, G. Bonura, S. Donato, S. Cavallaro, *Catal. Commun.*, **5**, 611 (2004).
13. I. Genova, T. Tsoncheva, M. Dimitrova, D. Paneva, B. Tsyntsarski, R. Ivanova, Z. Cherkezova-Zheleva, T. Budinova, D. Kovacheva, I. Mitov, N. Petrov, *Catal. Commun*, **55**, 43 (2014).
14. N. Velinov, E. Manova, T. Tsoncheva, Claude Estoumes, D. Paneva, K. Tenchev, V. Petkova, K. Koleva, B. Kunev, I. Mitov, *Solid State Sci.*, **14**, 1092 (2012).
15. K. Koleva, N. Velinov, T. Tsoncheva, I. Mitov,

Hyperfine Interact., **226**, 89 **(**2014).
16. N. Velinov, K. Koleva, T. Tsoncheva, E. Manova, D. Paneva, K. Tenchev, B. Kunev, I. Mitov, *Catal. Commun.*, **32**, 41 (2012).
17. W. Kraus, G. Nolze, PowderCell for Windows, Federal Institute for Materials Research and Testing, Berlin, 2000.
18. T. Žák, Y. Jirásková, CONFIT: Mössbauer Spectra fitting program, *Surf. Interface Anal*., **38**, 710 (2006).
19. E. Darezereshki, *Mater. Lett.*, **65**, 642 (2011).
20. M. V. Bukhtiyarova, A. S. Ivanova, E. M. Slavinskaya, L. M. Plyasova, V. A. Rogov, V. V. Kaichev, A. S. Noskov, *Fuel*, **90**, 1245 (2011).
21. I. A. Auwal, H. Güngüneş, A. Baykal, S. Güner, S. E. Shirsath, M. Sertkol, *Ceram. Int.*, **42**, 8627 (2016).
22. S. K. Chawla, R. K. Mudsainiyan, S. S. Meena, S. M. Yusuf, *J. Magn. Magn. Mater*., **350**, 23 (2014).
23. V. Šepelák, M. Myndyk, R. Witte, J. Röder, D. Menzel, R. H. Schuster, H. Hahn, P. Heitjans, K.-D. Becker, *Faraday Discuss*., **170**, 121 (2014).
24. M. Sorescu, A. Grabias, L. Diamandescu, D. Tarabasanu, *J. Mater. Synth. Process.*, **8**, 2 (2000).

СИНТЕЗ, СТРУКТУРА И КАТАЛИТИЧНИ СВОЙСТВА НА SrFe$_{12}$O$_{19}$ ХЕКСАФЕРИТ

К. В. Колева[1]*, Н. И. Велинов[1], И. Г. Генова[2], Т. С. Цончева[2], В. С. Петкова[3,4]

[1] *Институт по катализ, БАН, 1113 София, България*
[2] *Институт по органична химия с център по фитохимия, БАН, 1113 София, България*
[3] *Институт по минералогия и кристалография, БАН, 1113 София, България*
[4] *Нов български университет, 1618 София, България*

Постъпила на 16 януари 2018 г.; Преработена на 15 март 2018 г.

(Резюме)

Хексаферитната структура от М-тип (MeFe$_{12}$O$_{19}$) се състои от редуващи се шпинелни и хексагонални блокове, което поражда голямо разнообразие от разпределение на йоните в кристалната решетка. Елементарната клетка на този вид съединения е изградена от двувалентни алкалоземни метали Ca, Sr, Ba, а също така и метали от преходния ред (Co, Cu, Cr). Fe^{3+} йоните са разположени в пет кристалографски позиции: тетраедрична-FeO$_4$ (4f1), октаедрична-FeO$_6$ (12k, 2a, 4f2) и бипирамидална-FeO$_5$ (2b).

Цел на настоящото изследване е синтез на хексаферитни материали от М-тип (SrFe$_{12}$O$_{19}$) при ниска температура и контрол на размера на частиците чрез механохимично третиране, както и определяне на влиянието на структурните особености на образците върху техните каталитични свойства в реакция на разлагане на метанол.

Феритните материали са получени по метода на съутаяване с последваща термична обработка при 600 °C и 850 °C. На образец, получен при 850 °C, е приложено механично въздействие чрез смилане 1 и 5 часа. Образците са охарактеризирани с помощта на ДТА, рентгенофазов анализ и Мьосбауерова спектроскопия. Термично обработен при 850 °C образец е високо кристален SrFe$_{12}$O$_{19}$ хексаферит с наличие на втора фаза - хематит. Установено е редуциране на частиците по размер от 47 нм до 21 нм след един час механохимична обработка. Изследваните материали показват добра каталитична активност и селективност по CO в реакцията на разлагане на метанол. Образци, изследвани с Мьосбауерова спектроскопия след катализ, се отличават със стабилна хексаферитна фаза в силно редукционната среда на разлагане на метанол.